ALM: An Asperity-based Likelihood Model for California

Stefan Wiemer and Danijel Schorlemmer[1]
ETH Zürich, Switzerland

INTRODUCTION

In most earthquake hazard models, the *b*-value of the Gutenberg-Richter law plays a central role in forecasting future seismicity based on the observed history. The cumulative earthquake-size distribution is commonly described by a power law: $\log10(N) = a - bM$, where N is the cumulative number of earthquakes of magnitude M or greater, a is the earthquake productivity of a volume, and b is the relative size distribution (Gutenberg and Richter 1944; Ishimoto and Iida 1939). The slope of this power law, the *b*-value, is a critical parameter in seismology that describes the size distribution of events. A high *b*-value indicates a relatively larger proportion of small events, and vice versa.

In earthquake forecasting projects such as the source-related probabilistic seismic hazard assessment (PSHA), an underlying fundamental question is: What do the (numerous) smaller earthquakes tell us about the (infrequent) larger ones? Embedded into this question is also the question of stationarity: Can one trust recent small earthquakes to convey accurate information about infrequent large ones? It is these questions of scaling and stationarity that our model fundamentally addresses.

In PSHA projects, the *b*-value is either chosen as a regional constant or varies spatially between local zones. However, there is currently no obvious scientific basis for choosing either of these approaches. The model we propose, the Asperity-based Likelihood Model (ALM), assumes that the earthquake-size distribution, and specifically the *b*-value of recent micro-earthquakes, is the most important information for forecasting future events of **M** 5+. Below we first briefly review the evidence that leads us to propose the ALM model, and then we describe the actual steps involved in deriving the model parameters.

EVIDENCE FOR USING *b*-VALUES IN FORECASTING

Most of the evidence in support of ALM stems from observational data from a variety of tectonic regimes as well as from laboratory and numerical models. The literature on *b*-values is huge, and we will cite only a few articles, focusing on our own work over the past eight years. For an overview, we refer to the summary articles by Utsu (1999) and Wiemer and Wyss (2002).

The three strongest lines of evidence in support of ALM are summarized below.

1. The *b*-value of earthquakes has been shown to be inversely dependent on applied shear stress (Amitrano 2003; Scholz 1968; Schorlemmer *et al.* 2005b). Since stress/strain is the fundamental driving force of the earthquake process, we can make more precise, physics-based forecasts by using *b* as a stress meter within the Earth's crust where no direct measurements exist.
2. Asperities, locked patches of faults from which future earthquakes are likely to emanate, are found in many case studies to be characterized by low *b*-values (Schorlemmer and Wiemer 2005; Schorlemmer *et al.* 2004a; Schorlemmer *et al.* 2004b; Wiemer and McNutt 1997; Wyss 2001; Wyss *et al.* 2000). Creeping sections of faults where large ruptures are unlikely, on the other hand, often show *b*-values much higher than average (Amelung and King 1997; Wiemer and Wyss 1997; Wyss 2001).
3. Observational data from various tectonic regimes suggests that the *b*-value of micro-earthquakes, while spatially highly variable, is quite stationary with time (Schorlemmer *et al.* 2004a; Wiemer and Wyss 2002).

EVIDENCE FOR A UNIVERSAL INVERSE DEPENDENCE OF *b* ON DIFFERENTIAL STRESS

The *b*-value is spatially highly heterogeneous on all scales (Wiemer and Wyss 2002). Depending on the investigated data set, we find highly significant differences in *b* on scales of millimeters in laboratory samples, tens to hundreds of meters in volcanic or geothermal regions, kilometers in crustal anomalies observed by typical regional networks, and hundreds of kilometers on a global scale. We believe that research of the past eight years or so has clearly established that spatial *b*-value changes are highly significant and meaningful, and that earlier views that *b* is more or less a constant (Frohlich and Davis 1993; Kagan 1999) are wrong. We universally find that normal faulting events have the highest *b*-values, thrust events the lowest, and strike-slip events show intermediate values. The observed uniformity of the separation of *b*-values according to faulting type in different tectonic regimes suggests that the differential stress, and indirectly the confining pressure (to which the differential stress is tied), is the parameter most strongly controlling faulting types, thus influencing differences in *b*.

1. Now at University of Southern California, Department of Earth Sciences.

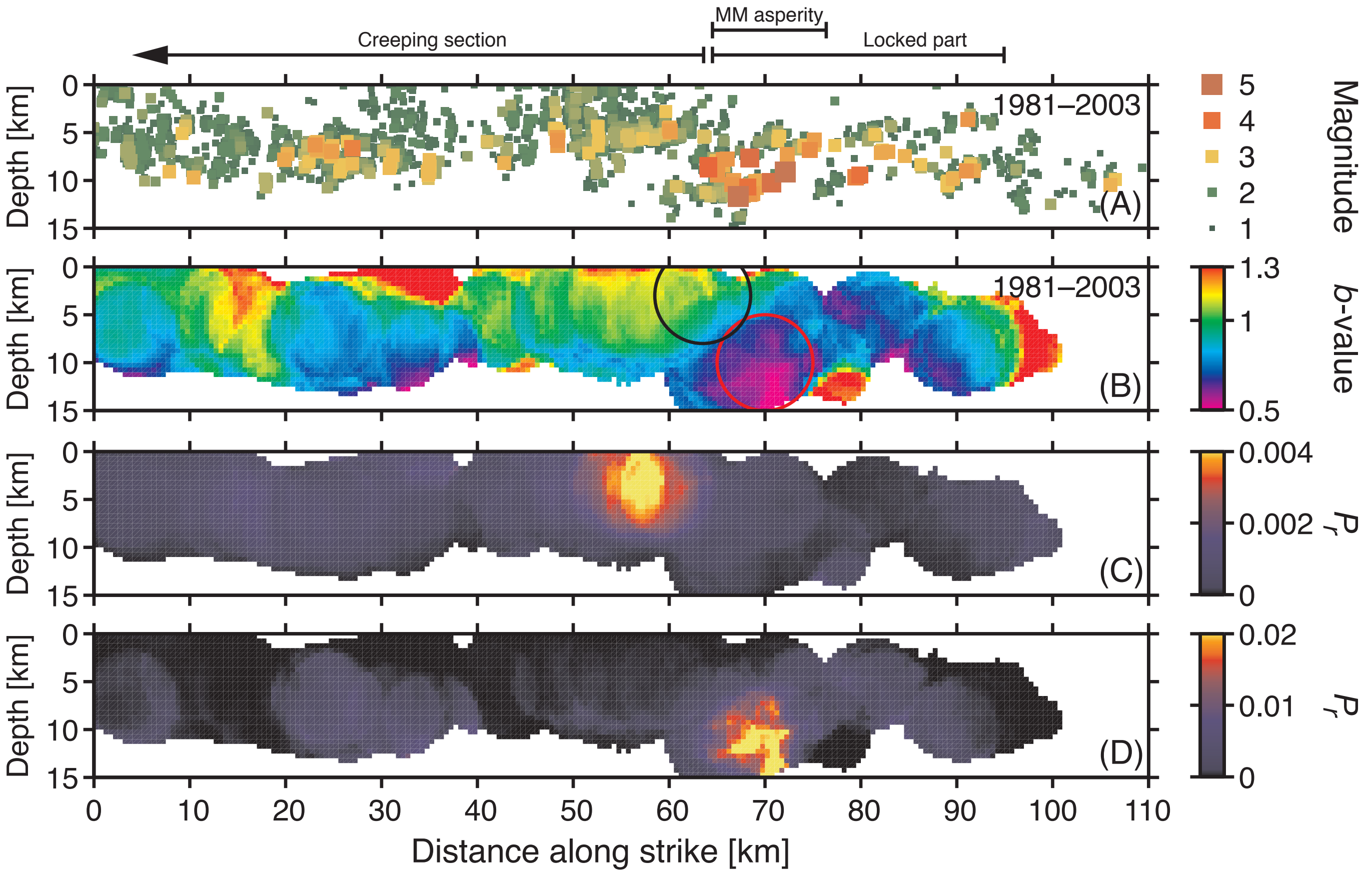

▲ **Figure 1.** NW–SE cross-sectional view along the San Andreas fault in the Parkfield region. (A) shows the seismicity from 1981 to 2005; size and color reflect the magnitude. (B) shows the *b*-value of the Gutenberg-Richter law, mapped using a constant radius of 5 km. Note the low *b*-values in the locked asperity region. (C) and (D) show the annual probability for **M** 6, (C) the first frame based on the assumption of an overall constant *b* of 0.91 and (D) the second using the above, spatially varying *b*-value distribution. In the case of Parkfield, we conclude that sensible hazard results are obtained only when taking into account spatial variations in *b* on the scale of kilometers.

MAPPING ASPERITIES USING *b*

The implications of strong spatial variability in *b* on earthquake probabilities is well illustrated when analyzing the Parkfield segment of the San Andreas fault (Wiemer and Wyss 1997). When mapping *b* in a cross-sectional view along the strike of the fault (figure 1) using volumes with radii of 5 km, we find that *b* in the Parkfield asperity is as low as 0.47 (volume A in figure 1), whereas it reaches values of up to 1.35 in the neighboring creeping section (volume B). In seismicity forecasts, we generally extrapolate the frequency-magnitude distribution (FMD) from the range of the observed data to the assumed upper maximum, M_{max}. Doing so for the FMDs of volumes A and B (as shown in figure 2) will yield very different results. If we compute for example the local probability for an **M** 6 or larger mainshock, we find a probability of about 0.02 for FMD A and on the order of 0.004 at location B (figure 1C and figure 2). The greatest hazard is thus found near the asperity, where the low *b*-value of < 0.5 produces the highest probability for an **M** 6 event. For comparison, we show the **M** 6+ forecast if the regional *b*-value of 0.9 is used at each node; hence only the *a*-value varies across the map. In this case, the creeping section of the fault has the highest hazard, because it is the most active (highest *a*-value). The two forecasts are distinctly different and our starting point for formulating ALM (Wiemer and Wyss 1997).

In early 2004, we analyzed the Parkfield segment in much more detail than Wiemer and Wyss (1997), focusing also on stationarity aspects of the *b*-values (Schorlemmer *et al.* 2004a; Schorlemmer *et al.* 2004b). We found that the *b*-value distribution remained remarkably stable with time, and that the seismicity in the years since Wiemer and Wyss (1997) clearly supported using a forecast model that uses spatially varying forecasts, with mapping radii of about 5 km giving the best results. The long-anticipated Parkfield event on 28 September 2004 subsequently occurred largely in areas of low *b*-values, in agreement with our conceptual model (Schorlemmer and Wiemer 2005). The ALM hypothesis has also been evaluated for several other faults in California, Japan, and Turkey, with generally good success (Oencel and Wyss 2000; Westerhaus *et al.* 2002;

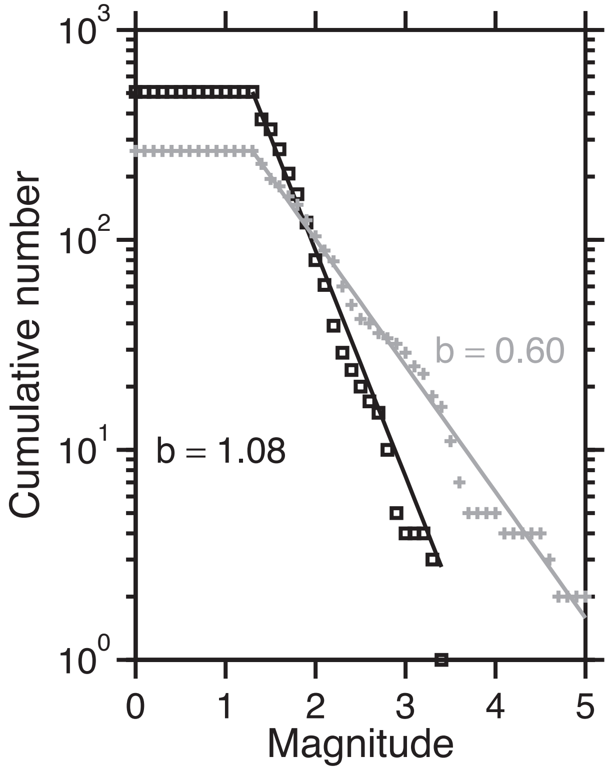

▲ **Figure 2.** Frequency-magnitude distributions obtained from the creeping section of the San Andreas fault (black) and the locked segment (gray).

Wyss and Matsumura 2001; Wyss *et al.* 2000). The challenge is to move from specific case studies to a systematic testing for a large region with much more heterogeneous properties.

THE ALM MODEL APPLIED TO CALIFORNIA

In computing a California-wide forecast based on the ALM hypothesis, we are faced with a number of decisions, such as: What mapping radii should we use? How do we treat depth? How do we deal with spatially variable completeness across California? How do we deal with clusters and swarms? What period should we use? Are there systematic magnitude differences between different regions? Should we apply smoothing? How do we best create a stable model?

Ideally, we would have calibrated the answers to these questions by setting up a complete search through the entire parameter space and maximizing the likelihood score. However, this would not only be computationally intense but also result in a model with a large number of free parameters to be tuned. While such a model would be well-tuned to retrospectively forecast seismicty, its ability to prospectively forecast may be disappointing. Therefore, we mostly used our intuition in the physical processes, based on the past case studies and tests, as guidelines, as described in more detail below. In some instances, we also have had to adopt simplifications, because, for example, cross-sectional mapping along faults is much more complex than mapping in latitudinal/longitudinal space. Below we briefly describe the rationale behind each decision step.

Microseismicity Catalog

We use the Advanced National Seismic System (ANSS) composite catalog (http://www.anss.org) for the period 1 January 1984–30 June 2005 as our baseline. Since the early 1980s, the seismic network configurations in California have been relatively stable and able to detect small events reliably. While changes in magnitude reporting do exist (Wyss and Wiemer 2000), they are to the best of our knowledge relatively minor. One problem for our analysis is the fact that magnitude scales for magnitude 1–4 events used in southern and northern California differ. This can lead to systematically different forecasts of the number of **M** 5+ events, which are given as moment magnitudes. Addressing this problem is nontrivial and thus not possible within the scope of this study. Location uncertainty is another possible source of error in our analysis. Ideally, we like to use relocated catalogs, but no such catalog was available to us for northern California, and the task of patching together one composite catalog is nontrivial. Because in past studies we found that location accuracy has a minor influence on *b*-value estimates on the scales that we are interested in (Woessner *et al.* 2005), we use the standard network locations for our estimation.

Declustering the Catalog

Many earthquakes are part of sequences, such as swarms or aftershock sequences. Our attempt to forecast the average expected rate of **M** 5+ events could be significantly biased if our rate estimation at a given location included a rich aftershock sequence of a moderate to large mainshock. Removing earthquake clusters, or declustering (Gardner and Knopoff 1974; Reasenberg 1985), is an imperfect attempt to correct for this bias by removing dependent events from the catalog. Declustering is not a unique process because there is no unique definition of dependent events. In full awareness of the shortcomings of declustering, we select the approach proposed by Uhrhammer (1986) because of its simplicity. Declustering the entire ANSS catalog using Reasenberg's approach is challenging, because this process is slow and completeness varies spatially.

Estimating Completeness

The parameter most critical for an accurate determination of the *b*-value (and, in our model, also the *a*-value) is the completeness, M_c. We need an accurate description of the local M_c. Because M_c for the forecast regions varies between below 1 to above 3, we cannot afford to work with an overall M_c cut, as we would lose > 99% of the available events for mapping. Fortunately, M_c can be derived quite accurately from the observed data when assuming a power law distribution—the loss of detection at the lower magnitude end can be well modeled (Wiemer and Wyss 2000; Woessner and Wiemer 2005). Using the entire magnitude range (EMR) method (Woessner and Wiemer 2005), which performs a bootstrap estimate of M_c and its uncertainty, we compute an M_c model for the study region (figure 3). We add 0.2 at

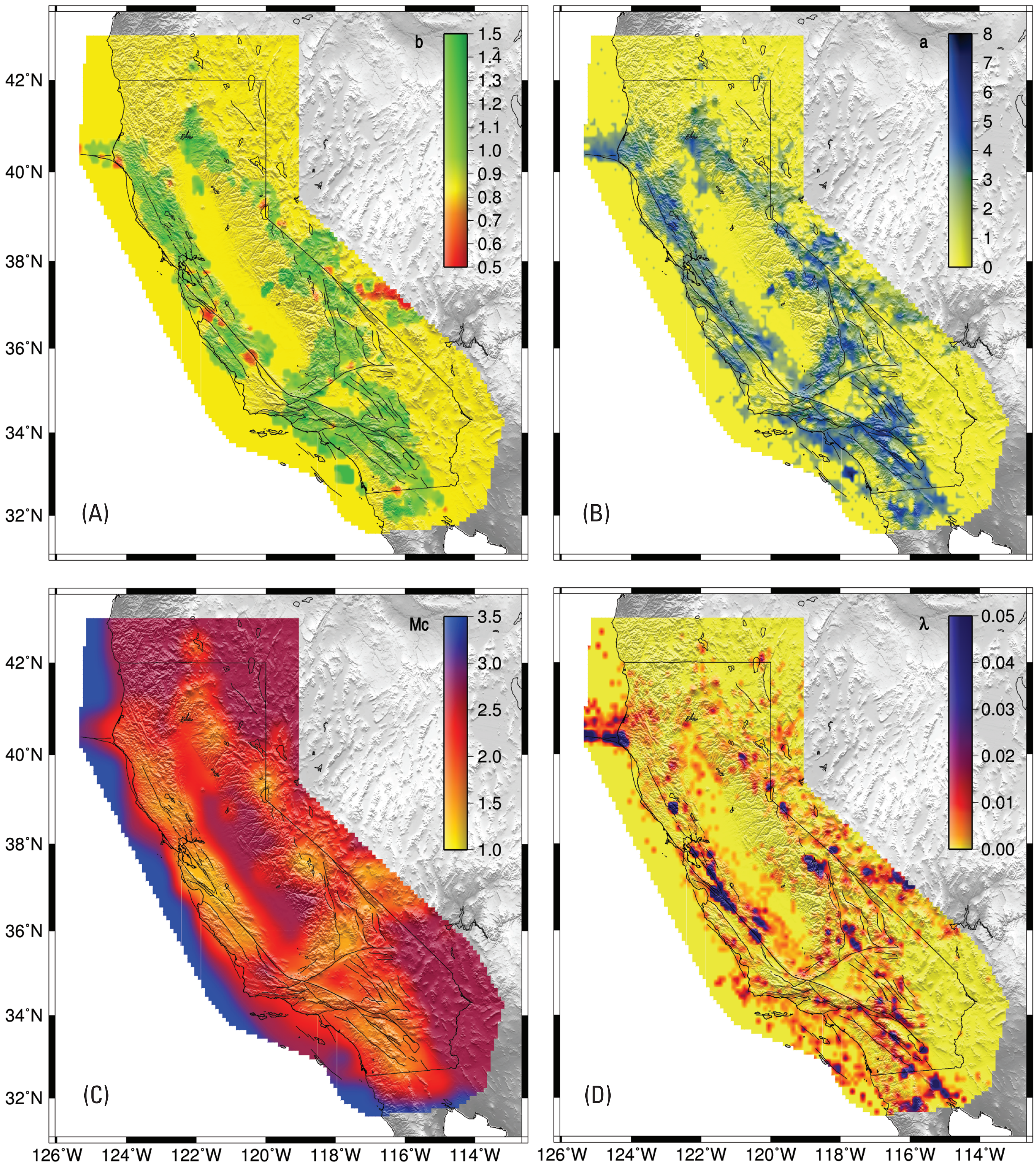

▲ **Figure 3.** Maps of (A) *b*-values, (B) *a*-values, (C) magnitude of completeness, M_c, and (D) the forecast for **M** ≥ 5 events of our model.

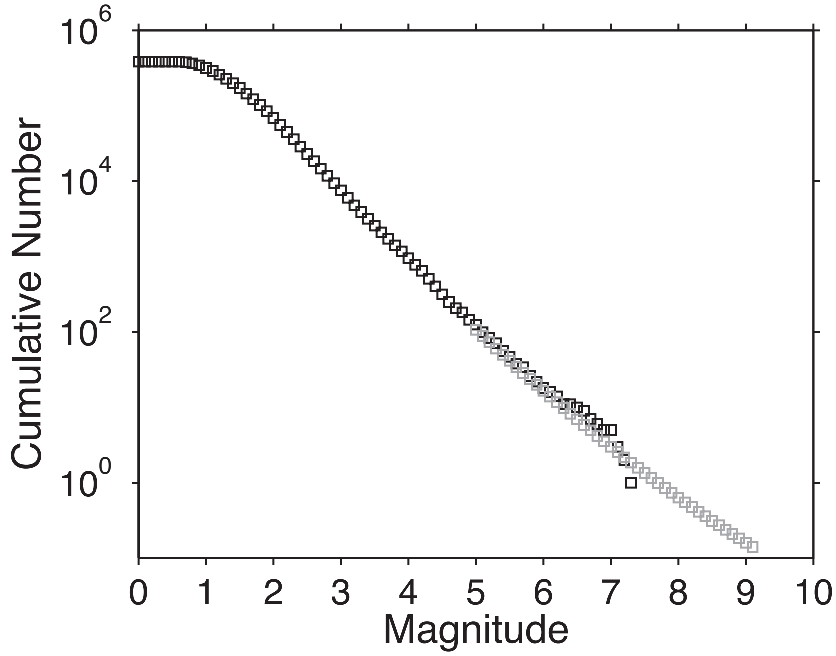

▲ **Figure 4.** Frequency-magnitude distributions of the declustered catalog used for computing the forecast (black) and of the forecast of our model normalized to the catalog's time period (gray).

each node as an extra safety factor and smooth the model using a Gaussian kernel.

Regional *b*-value

In nodes with insufficient data, as explained below, we default to using a regional *b*-value estimate instead of a local one. Using the entire data set above $M_c = 3.5$, we estimate this regional *b*-value for California to be $b = 0.823$, which is in good agreement with the estimate by Knopoff (2000).

Spatial Resolution and Rate Estimation

The spatial resolution at which we are able to map asperities in our method depends critically on the density of available data. For small sample sizes, the *b*-value estimation is highly uncertain and a forecast is likely to be unstable. In such situations, the regional *b*-value should be selected as the preferred model. The suitable mapping resolution, however, also depends on the scaling of the underlying stress heterogeneity that is associated with asperities. In past studies at Parkfield and Morgan Hill (Wiemer and Wyss 1997), we found that a 5-km radius is well suited to map asperities associated with **M** 6–type events. For the San Jacinto and Elsinore faults, seismicity rates are lower and larger radii of 20 km had to be used (Wyss *et al.* 2000). Because the density of earthquakes across California is highly variable, we believe that using a constant box or radius across the entire map is not satisfactory. We thus choose a nested approach, allowing for increasing radii if not enough events are available locally.

The *b*-value and *a*-value are estimated using the commonly applied maximum likelihood estimation method, using the specified M_c at each location. To test if the seismicity above the local M_c in a given 0.1 × 0.1 degree square (defined in the Regional Earthquake Likelihood Models (RELM) testing setup; Schorlemmer and Gerstenberger 2007, this issue) warrants a local estimate rather than a global one, we evaluate two models. In model A, we estimate a local *b*-value. This model has one degree of freedom. In model B, we use a regional *b*-value (zero degrees of freedom). We then measure the relative goodness of fit to the data. The fit of each model to the observed data is computed as a likelihood score (Aki 1965); however, because the models have different degrees of freedom (*i.e.*, free parameters), these likelihood scores cannot be compared directly. To select between the two models we use the corrected Akaike Information Criterion, $\mathrm{AIC_c}$ (Kenneth *et al.* 2002):

$$\mathrm{AIC_c} = -2\max\left(\ln L\right) + 2\left(P\right) + \frac{2P\left(P+1\right)}{N-P-1}$$

with $\log L(a, b)$ being the log-likelihood function, P the number of free parameters, and N the sample size. In contrast to the original Akaike Information Criterion (Akaike 1974; Imoto 1991; Ogata 1999), the corrected $\mathrm{AIC_c}$ corrects for the sample size, which becomes critical for small sample sizes. The model with the lowest $\mathrm{AIC_c}$ is the preferred model. We then couple the model selection to the problem of spatial resolution, searching for the smallest sample sizes where a local model forecasts better than the global one. We use the following approach:

- If the $\mathrm{AIC_c}$ of the local estimate of b is lower than the regional one, we use this lower *b*-value and estimate the respective *a*-value for this node.
- If the regional $\mathrm{AIC_c}$ is lower, we increase the sampling radius in 1-km steps, starting at 7 km to a maximum of 20 km. We use the local *b*-value for the smallest radii where the local *b*-value model scores a lower $\mathrm{AIC_c}$. The *a*-value

at this node is then computed from the seismicity in the square-testing node, prescribing the local b-value.

- If at the maximum radius of 20 km the regional b-value still has a lower AIC_c score, we use it and no local estimate.
- If we have no event at all in such a node, we define a "water line" by assuming an a-value of −2 at $M = 0$.

Depth

We consider all events down to 30-km depth for making the forecast, because this is the depth range to be addressed in the RELM test.

Smoothing

Smoothing reflects the degree of trust we have in the resolution and the stationarity of the model. Many seismicity-based models use smoothing, generally smoothing the a-value or forecast. Because in our approach b-value and M_c also vary quite strongly, it would be easiest to smooth the final rate forecast at each node and for each magnitude bin. However, because the testing hypocenter accuracy is integrated already (Schorlemmer and Gerstenberger 2007, this issue), we feel that additional smoothing is not needed, since the testing volumes are already quite large.

Maximum Magnitude

The maximum magnitude, $M_{max,}$ is poorly understood, and our approach offers no insight into its determination. Therefore, we choose M_{max} to be the upper limit of the test range ($M = 9.0$; Schorlemmer and Gerstenberger 2007, this issue). Note that the forecasted rates of large events at low seismicity nodes are very low; however, by not limiting M_{max} our model will likely produce unrealistically high moment releases (Hough 1996) and unrealistically high hazard for longer return periods where the larger events control the hazard. The RELM test for which this model was primarily developed has no ability to resolve the M_{max} issues because the M_{max} return times in California are hundreds of years or more. To explore hazard implications of the ALM model, we propose to limit the M_{max} at each node based on expert estimates, preferentially using a logic-tree approach to reflect the large uncertainty in $M_{max.}$

THE FINAL MODEL

Having established for each node of the testing grid an a-value and b-value, we forecast the annual rate of events in each magnitude bin $5.0 \leq \mathbf{M} \leq 9.0$. The cumulative rate of $M \geq 5.0$ events, forecasted for a five-year period, is shown in figure 3. Our model predicts a total of 23.7 events for the entire forecast region for the period 2006–2010. Differences between neighboring nodes can be quite strong, resulting from the fact that we did not smooth our forecasts. In figure 4 we validate that our summed forecast is in agreement with the declustered, observed seismicity of the past 20 years. Note that we forecast higher rates of **M** 8+ than observed, which is a result of the fact that (1) truly large events have not occurred in the past 20 years; and (2) in our low b-value zones, we forecast quite high rates of **M** 9, which may be unrealistic and a result of our simplistic choice of M_{max}. The ALM model has been submitted for prospective testing to the RELM test center (Schorlemmer *et al.* 2007, this issue) starting 1 January 2006. The code to produce the ALM model is freely available via the RELM Web site, `http://www.relm.org`.

The ALM model allows for a first systematic regional test of the hypothesis that the strong spatial variations in b-values are meaningful for forecasting future seismicity. Future refinements of ALM might include a more sophisticated treatment of depth, mapping along cross-sections, a higher resolution mapping, and the introduction of different M_{max} values. Despite these limitations, we believe that the results of prospective testing will be highly valuable in guiding our understanding of the physics of b-values and forecasting of seismicity. We wish our model all the best in the upcoming five-year prospective testing.

ACKNOWLEDGMENTS

The authors would like to thank Jochen Woessner for providing a detailed M_c model for the study region and for advice on declustering. We thank Ned Field for his support and dedication to RELM throughout the years and Sue Hough and an anonymous reviewer for helpful suggestions on how to improve this manuscript. This research was supported by the Southern California Earthquake Center (SCEC), which is funded by NSF Cooperative Agreement EAR-0106924 and USGS Cooperative Agreement 02HQAG0008. The SCEC contribution number for this paper is 1000. The Geophysical Institute of ETH Zürich contribution number is 1450.

REFERENCES

Akaike, H. (1974). New Look at Statistical-Model Identification, *IEEE Transactions on Automatic Control,* AC19 (6), 716–723.

Aki, K. (1965). Maximum likelihood estimate of b in the formula $\log N = a - bM$ and its confidence limits: *Bulletin of the Earthquake Research Institute* **43**, 237–239.

Amelung, F., and G. King (1997). Earthquake scaling laws for creeping and non-creeping faults. *Geophysical Research Letters* **24**, 507–510.

Amitrano, D. (2003). Brittle-ductile transition and associated seismicity: Experimental and numerical studies and relationship with the b value. *Journal of Geophysical Research—Solid Earth* **108**, art. no. 2,044.

Frohlich, C., and S. Davis (1993). Teleseismic b-values: Or, much ado about 1.0. *Journal of Geophysical Research—Solid Earth* **98**, 631–644.

Gardner, J. K., and L. Knopoff (1974). Is the sequence of earthquakes in Southern California, with aftershocks removed, Poissonian? *Bulletin of the Seismological Society of America* **64**, 1,363–1,367.

Gutenberg, B., and C. F. Richter (1944). Frequency of earthquakes in California. *Bulletin of the Seismological Society of America* **34**, 185–188.

Hough, S. E. (1996). The case against huge earthquakes. *Seismological Research Letters* **67**, 3–4.

Imoto, M. (1991). Changes in the magnitude frequency b-value prior to large (M-greater-than-or-equal-to-6.0) earthquakes in Japan. *Tectonophysics* **193**, 311–325.

Ishimoto, M., and K. Iida (1939). Observations of earthquakes registered with the microseismograph constructed recently. *Bulletin of the Earthquake Research Institute* **17,** 443–478.

Kagan, Y. (1999). Universality of the seismic moment-frequency relation. *Pure and Applied Geophysics* **155**, 537–574.

Kenneth, P., K. P. Burnhaman, and D. R. Anderson (2002). *Model selection and multimodel inference: A practical information—Theoretic Approach,* Springer, New York.

Knopoff, L. (2000). The magnitude distribution of declustered earthquakes in Southern California. *Proceedings of the National Academy of Sciences of the United States of America* **97**, 11,880–11,884.

Oencel, A.O., and M. Wyss (2000). The major asperities of the $M_w = 7.4$ Izmit earthquake, defined by the microseismicity of the two decades before it. In *The Izmit and Duzce Earthquakes: Preliminary Results*, ed. A. Barka, O. Kozacπ, S. Akyüz, and E. Altunel, 1–4. Istanbul: Istanbul Technical University.

Ogata, Y. (1999). Seismicity analysis through point-process modeling: A review. *Pure and Applied Geophysics* **155**, 471–507.

Reasenberg, P. A. (1985). Second-order moment of Central California seismicity. *Journal of Geophysical Research* **90**, 5,479–5,495.

Scholz, C. H. (1968). The frequency-magnitude relation of microfracturing in rock and its relation to earthquakes, *Bulletin of the Seismological Society of America* **58**, 399–415.

Schorlemmer, D., and M. C. Gerstenberger (2007). RELM Testing Center. *Seismological Research Letters* **78,** 30–36.

Schorlemmer, D., M. C. Gerstenberger, S. Wiemer, D. D. Jackson, and D. A. Rhoades (2007). Earthquake Likelihood Model Testing. *Seismological Research Letters* **78,** 17–29.

Schorlemmer, D., and S. Wiemer (2005). Microseismicity data forecast rupture area. *Nature* **434**, 1,086.

Schorlemmer, D., S. Wiemer, and M. Wyss (2004a). Earthquake statistics at Parkfield: 1. Stationarity of *b* values. *Journal of Geophysical Research—Solid Earth* **109**, B12307, doi:10.1029/2004JB003234.

Schorlemmer, D., S. Wiemer, and M. Wyss (2005b). Variations in earthquake-size distribution across different stress regimes. *Nature* **437**, 539–542.

Schorlemmer, D., S. Wiemer, M. Wyss, and D. D. Jackson (2004b). Earthquake statistics at Parkfield: 2. Probabilistic forecasting and testing. *Journal of Geophysical Research—Solid Earth*, **109**, B12308, doi:10.1029/2004JB003235.

Uhrhammer, R. (1986). Characteristics of northern and southern California seismicity. *Earthquake Notes* **57**, 21.

Utsu, T. (1999). Representation and analysis of the earthquake size distribution: A historical review and some new approaches. *Pure and Applied Geophysics* **155**, 509–535.

Westerhaus, M., M. Wyss, R. Yilmaz, and J. Zschau (2002). Correlating variations of *b* values and crustal deformations during the 1990s may have pinpointed the rupture initiation of the Mw = 7.4 Izmit earthquake of 1999 August 17. *Geophysical Journal International* **148**, 139–152.

Wiemer, S., and S. McNutt (1997). Variations in frequency-magnitude distribution with depth in two volcanic areas: Mount St. Helens, Washington, and Mt. Spurr, Alaska. *Geophysical Research Letters* **24**, 189–192.

Wiemer, S., and M. Wyss (1997). Mapping the frequency-magnitude distribution in asperities: An improved technique to calculate recurrence times? *Journal of Geophysical Research* **102**, 15,115–15,128.

Wiemer, S., and M. Wyss (2000). Minimum magnitude of complete reporting in earthquake catalogs: Examples from Alaska, the western United States, and Japan. *Bulletin of the Seismological Society of America* **90**, 859–869.

Wiemer, S., and M. Wyss (2002). Mapping spatial variability of the frequency-magnitude distribution of earthquakes. *Advances in Geophysics* **45**, 259–302.

Woessner, J., D. Schorlemmer, S. Wiemer, and P. M. Mai (2006). Spatial correlation of aftershock locations and on-fault main shock properties, *Journal of Geophysical Research* **111**, doi:10.1029/2005JB003961.

Woessner, J., and S. Wiemer (2005). Assessing the quality of earthquake catalogues: Estimating the magnitude of completeness and its uncertainty. *Bulletin of the Seismological Society of America* **95**, 684–698.

Wyss, M. (2001). Locked and creeping patches along the Hayward fault, California. *Geophysical Research Letters* **28**, 3,537–3,540.

Wyss, M., and S. Matsumura (2002). Most likely locations of large earthquakes in the Kanto and Tokai areas, Japan, based on the local recurrence times, *Physics of the Earth and Planetary Interiors* **131**, 173–184.

Wyss, M., D. Schorlemmer, and S. Wiemer (2000). Mapping asperities by minima of local recurrence time: The San Jacinto-Elsinore fault zones. *Journal of Geophysical Research* **105**, 7,829–7,844.

Wyss, M., and S. Wiemer (2000). Change in the probability for earthquakes in Southern California due to the Landers magnitude 7.3 earthquake. *Science* **290**, 1,334–1,338.

ETH Zürich
Schafmattstr. 3
8093 Zürich, Switzerland
stefan@sed.ethz.ch
(S.W.)

University of Southern California
Department of Earth Sciences
3651 Trousdale Parkway, MC-0740
Los Angeles, California 90089-0740 USA
danijel@usc.edu
(D.S.)